

Cephalosoma Detection using Double Multilayer Back propagation Neural Network

D.Selvaraj¹, R.Dhanasekaran²

Research Scholar, Dept. of ECE, Sathyabama University¹
Dean, Research, Syed Ammal Engineering College²,
Email: mails2selvaraj@yahoo.com, rdhanasekar@yahoo.com²

Abstract—In our proposed method, an automatic cephalosoma segmentation and classification system is developed. The input image is preprocessed, segmented and features are extracted. Based on the extracted features, the input image is classified as cephalosomous or non-cephalosomous image using multilayer back propagation neural network classifier. In the preprocessing stage, noise is removed using median filter and the skull is stripped using morphological operators. Using thresholding technique and orthogonal polynomial transform, the skull stripped image is segmented into gray matter, white matter, cerebrospinal fluid and tumour. Then features like mean, variance, energy, and entropy are calculated. Later, multilayer back propagation neural network (MLBPNN) is trained with extracted features. A total of 150 images have been used, out of which 60 are used for training and remaining 90 images for testing. MLBPNN classifier classifies the input image to be cancer affected or normal based on features extracted. If the image is cancer affected, then type of cancer is detected as malign tumor or benign tumor using another MLBPNN Classifier.

The performance of the proposed technique is validated and compared with the standard evaluation metrics such as sensitivity, specificity and accuracy values for neural network. The proposed method is compared with two standard methods KNN and FCM+NN. The obtained result depicts that the proposed classification method yields better results.

Index Terms—Brain Segmentation, Cephalosoma, Feature Extraction, Neural Network, Brain Tumour.

I. INTRODUCTION

The primary goal of MRI brain image segmentation is to partition a given brain image in to true anatomical structures representing such as grey matter, white matter, cerebrospinal fluid, skull and scalp. Later, the abnormalities in these tissues are detected. Identification and segmentation of brain tumor in magnetic resonance images is very crucial in medical diagnosis because it gives information related to anatomical structures as well as potential abnormal tissues necessary for treatment planning and patient follow-up. Precise segmentation of brain tumor is also useful for general modeling of

pathological brains as well as the creation of pathological brain atlases [16, 17].

There is a significant inter-patient variation of signal intensities for the same tissues [3]. Although there are several approaches for MRI Brain image segmentation: discriminant analysis [5], neural networks [6,7], clustering [4], brain atlases [8], knowledge-based techniques [9], shape-based models [10,11], morphological operators [12], multivariate principal component analysis [13], pixel based models like Expectation Maximization Algorithm [14], Multi-resolution edge detection [6] and statistical pattern recognition [15], to name a few. Precise segmentation and classification of abnormalities are still a challenging and complicated task because of inherent noise, partial volume effect, different shapes, locations and image intensities of different types of tumors.

Manual segmentation cannot be compared with the current high speed computing machines that allow us to visually observe the size and position of the superfluous tissues. Supervised segmentation methods have exhibited problems with reproducibility, due to significant intra and inter-observer variance introduced over multiple trials of training Furthermore; they are time consuming and require domain experts. Whereas, the accuracy of unsupervised segmentation methods are less and depend upon input image. So these limitations suggest the need for a fully automatic method for segmentation.

In this paper, we have presented an efficient detection technique for the tumor region in the Brain MRI images. Here, we have utilized the brain tissue segmentation technique that we have proposed in our previous research paper [1, 2, 19, 20]. In addition with that, we have detected the tumor region with the aid of the regionprops algorithm [18]. Subsequently, the features vectors of all the segmented regions of the brain MRI image are calculated. Then, the abnormality classification is carried out by means of multilayer backpropagation neural network.

The rest of this paper is organized as follows: section 2 presents our proposed Brain tissues segmentation

technique. Extractions of features from the segmented tissues are explained in section 3. Section 4 explains the classification of the input image using MLPNN. The detailed experimental results and discussions are given in section 5. At last, section 6 concludes the paper.

II. PROPOSED METHOD

The block diagram of the proposed technique is shown in Fig 1. Our proposed method consists of 4 phases namely preprocessing, segmentation, feature extraction and classification. In preprocessing phase, the noise is removed using median filter and the skull is stripped using morphological operators and thresholding technique. Later, the skull stripped image is segmented into gray matter and white matter using thresholding technique. Orthogonal polynomial transform is used to segment cerebrospinal fluid. After segmentation process, the features such as Mean, Variance, Energy and Entropy are extracted from the regions and given to the MLPNN classifier for training. Later, the image is classified as tumorous or normal with the help of trained MLPNN. Finally, the type of cancer is detected using another MLPNN classifier.

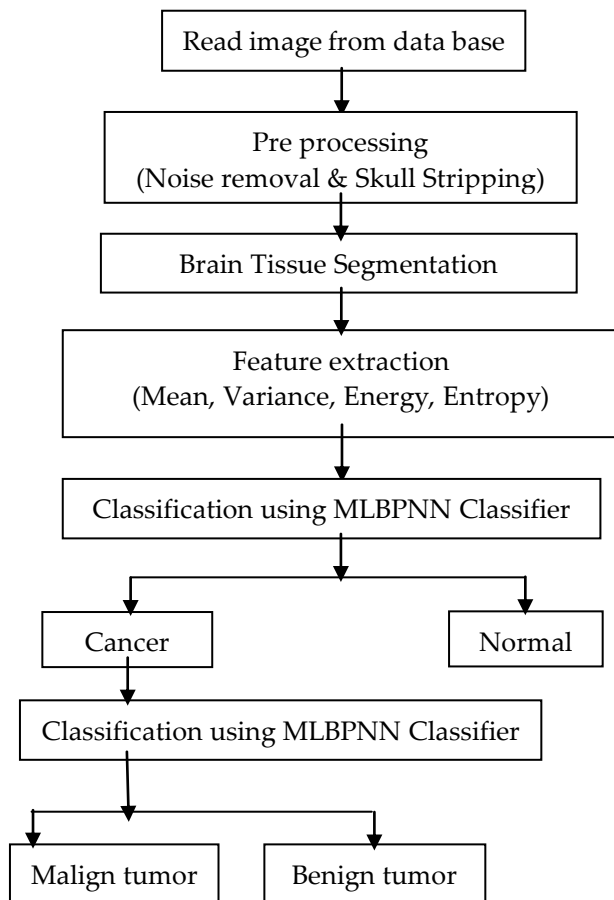


Figure 1: Block diagram of proposed approach

The obtained experimental results by our proposed

technique in our previous research paper [1, 2, 19, 20] are as shown in Fig 2 and Fig 3. Here, we have given all the outcomes of the input image with and without tumour region.

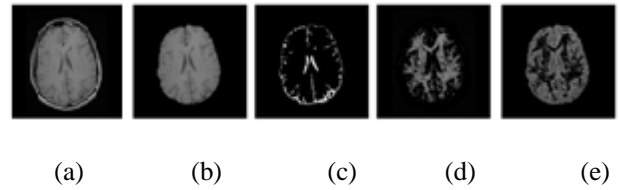


Figure 2: Segmented results of Brain MRI without tumor. (a) Input Brain MRI image, (b) Skull stripped image, (c) Cerebrospinal fluid image, (d) White matter, (e) Gray matter

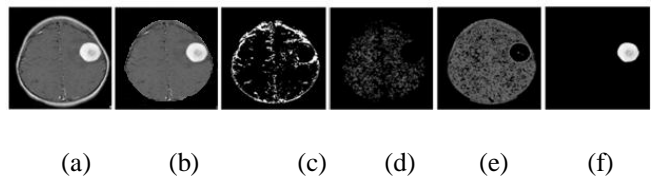


Figure 3: Segmented results of Brain MRI with tumor. (a) Input Brain MRI image, (b) Skull stripped image, (c) Cerebrospinal fluid image, (d) White matter, (e) Gray matter, (f) Tumor region

III. FEATURE EXTRACTION FROM THE SEGMENTED TISSUES

The analyzing methods have been done so far has used the values of pixels intensities, pixels coordinates and some other statistic features namely mean, variance or median, which have much error in determination process and low precision and efficiency in classification [19]. Here, the statistic features we have chosen are Mean M , Variance σ^2 , Entropy E and Energy $E_{(E,V,D)}$ functions. The feature extraction process is carried out with some initial pre-processing. Each tissue segmented image is split into a limited number of blocks and the feature values are calculated for every block. The block diagram of the feature extraction process is given in Fig. 4. The initial steps are as follows:

- Find the neighbor blocks of the entire divided blocks.
- Find the distance between all the neighbor blocks.
- Find the feature values of the blocks with distinct distance measure.
- Find the average value of all the computed blocks' distance.
- Store all the features in a vector and fed as an input to the classifier.

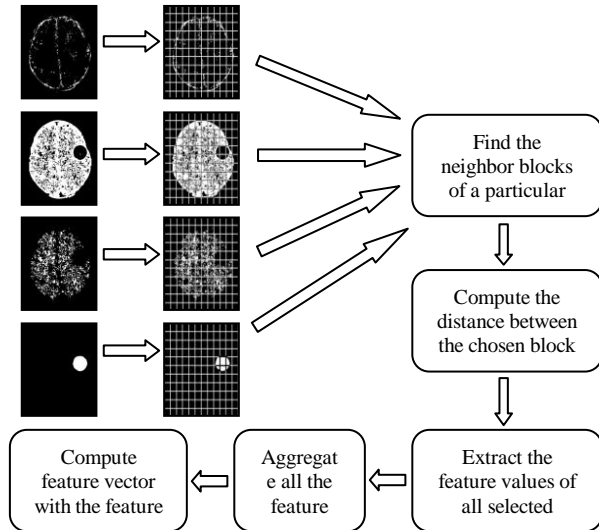


Figure 4: Block diagram of Feature extraction process
The statistic feature's formula is depicted as below,

$$\text{Mean, } M = \frac{1}{mn} \sum_{i=1}^m \sum_{j=1}^n x(i, j) \quad (1)$$

$$\text{Variance, } \sigma^2 = \frac{1}{mn} \sum_{i=1}^m \sum_{j=1}^n (x(i, j) - M)^2$$

$$\text{Entropy, } E = - \sum_i \sum_j x(i, j) \log x(i, j) \quad (2)$$

$$\text{Energy, } E_{(H,V,D)} = \sum_i \sum_j x(i, j)^2 \quad (3)$$

Selection of efficient features can reduce significantly the difficulty of the classifier design. The obtained trained feature is compared with the test sample feature obtained and classified as one of the extracted features. The training feature vector F_v is defined by combining all the extracted features like mean M , variance σ^2 , entropy E and the energy $E_{(H,V,D)}$. In order to obtain the three wavelet energies, the Haar wavelet transform is applied to each blocks of brain MRI image. After a one level wavelet transform, a 4×4 pixel block is decomposed into four frequency bands of 2×2 coefficients. For example, the coefficients in horizontal band of one block are H_1, H_2, H_3, H_4 , in vertical band V_1, V_2, V_3, V_4 and in diagonal band D_1, D_2, D_3 and D_4 . Then horizontal energy E_H , vertical energy E_V and diagonal energy E_D are combined to attain the feature value of the energy.

$$\text{Feature Vector, } F_v = [f(M), f(\sigma^2), f(E), f(E_H), f(E_V), f(E_D)] \quad (5)$$

IV. BRAIN IMAGE CLASSIFICATION USING MLBPNN

The classifiers we have used here is MLBPNN. The general structure of MLBPNN is shown in fig. 5. In this

network, the information moves in only one direction, forward from input layer to the output layer through the hidden layers. The network consists of 1 input layer with 24 neurons, 1 output layer with one neuron and 2 layers of hidden units with 10 neurons. The algorithm used to train the network is back propagation algorithm.

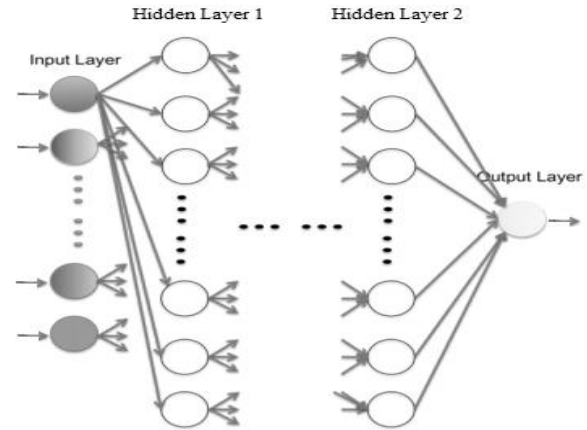


Figure 5: General Structure of MLBPNN

Each hidden node calculates the weighted sum of its inputs and applies a thresholding function to determine the output of the hidden node. The weighted sum of the inputs for hidden node Z_h is calculated as,

$$Z_h = \sum_{i=0}^n W_{hi} X_i \quad (6)$$

The thresholding function applied at the hidden node is a sigmoid function. The general form of the sigmoid function is

$$\text{Sigmoid}(a) = \frac{1}{1 + e^{-a}} \quad (7)$$

The sigmoid function is also called as squashing function, because it squashes its input to a value between 0 and 1. At the hidden node, the sigmoid function is applied to the weighted sum of the inputs to the hidden node. So, the output of hidden node is given as,

$$Z_h = \text{Sigmoid} \left(\sum_{i=0}^n W_{hi} X_i \right) = \frac{1}{1 + e^{-\sum_{i=0}^n W_{hi} X_i}} \quad (8)$$

Similar computation is done for the next hidden and output units. We have only one output unit in the output layer. So, the following sigmoid function (equation 8) is applied to the output unit.

$$y = \text{Sigmoid} \left(\sum_{h=0}^N V_h Z_h \right) = \frac{1}{1 + e^{-\sum_{h=0}^N V_h Z_h}} \quad (9)$$

The algorithm used to train the neural network is backpropagation algorithm. This algorithm uses gradient descent to update the weights so as to minimize the squared error between the network output values and the target output values. The update rules are derived by taking the partial derivative of the error function with

respect to the weights to determine each weight's contribution to the error. Then, each weight is updated using gradient descent according to its contribution to the error. The weight update of our network is given in equation (10).

$$\Delta v_h = \eta(r^t - y^t)z_h^t \quad (10)$$

$$\Delta w_{hi} = \eta(r^t - y^t)v_h z_h^t (1 - z_h^t)x_i^t \quad (11)$$

Where, 't' is the current input and 'η' is the learning rate. Its value is set to 0.1. The error produced by the network is calculated using the error function

$$E(W, v | x^t, r^t) = \frac{1}{2}(r^t - y^t)^2 \quad (12)$$

V. EXPERIMENTAL RESULTS AND DISCUSSION

We have presented a technique for segmentation and detection of pathological tissues (Tumor), normal tissues (White Matter and Gray Matter) and fluid (Cerebrospinal Fluid) from magnetic resonance (MR) images of brain with the help of composite feature vectors comprising of wavelet and statistical parameters. The proposed technique can successfully segment the tumors as well as the brain tissues, provided that the parameters are set properly. The proposed technique is designed for supporting the tumor detection in brain images with tumor and without tumor. The obtained experimental results from the proposed technique are given in Fig. 6 and Fig. 7. In fig. 6 and fig. 7, the segmented normal tissues (CSF, WM, and GM) and pathological tissues (tumour) of MRI brain image with and without tumor is shown. The feature values calculated for these segmented tissues using block based feature extraction method is tabulated in table 1. The simulation result of neural network training dataset is as shown in Fig 8 to Fig 11.

| Image No. | Input Image | Cerebrospinal Fluid (CSF) | Gray Matter (GM) | White Matter (WM) | Tumour |
|-----------|-------------|---------------------------|------------------|-------------------|--------|
| AN1 | | | | | |
| AN2 | | | | | |
| AN3 | | | | | |
| AN4 | | | | | |
| AN5 | | | | | |
| AN6 | | | | | |

Figure 6: Segmented normal tissues (CSF, GM, WM) and pathological tissues(tumor) of mri brain images with tumor

| Image No. | Input Image | Cerebrospinal Fluid (CSF) | Gray Matter (GM) | White Matter (WM) |
|-----------|-------------|---------------------------|------------------|-------------------|
| N1 | | | | |
| N2 | | | | |
| N3 | | | | |
| N4 | | | | |

Figure 7: Segmented normal tissues (CSF, GM, WM) and pathological tissues(tumor) of mri brain images without tumor

TABLE 1
Feature values extracted from segmented tissues of MRI brain images

| Image No. | Tissue | Feature Values | | | | | |
|-----------|--------|----------------|---------|------|---------|---------|-------|
| | | Mean | Var | Ent | Energy | | |
| | | | | | Hori z. | Verti . | Diag. |
| AN1 | CSF | 0.43 | 0.157 | 0.74 | 1.67 | 1.60 | 1.32 |
| | GM | 68.41 | 819.28 | 0.43 | 12.62 | 12.18 | 9.67 |
| | WM | 33.9 | 1311.07 | 0.73 | 15.73 | 15.22 | 13.05 |
| | Tumor | 180.4 | 1609.4 | 0.3 | 20.9 | 12.20 | 7.2 |
| AN2 | CSF | 0.46 | 0.14 | 0.68 | 1.63 | 1.60 | 1.34 |
| | GM | 66.87 | 946.97 | 0.47 | 13.31 | 12.49 | 10.2 |
| | WM | 37.13 | 1369.71 | 0.72 | 15.92 | 15.00 | 13.01 |
| | Tumor | 181.48 | 935.04 | 0.18 | 12.68 | 11.77 | 7.80 |
| AN3 | CSF | 0.51 | 0.14 | 0.67 | 1.58 | 1.53 | 1.14 |
| | GM | 69.40 | 861.86 | 0.43 | 12.94 | 11.94 | 9.62 |
| | WM | 35.48 | 1315.72 | 0.72 | 16.04 | 15.07 | 13.01 |
| | Tumor | 151.10 | 829.26 | 0.22 | 12.21 | 11.79 | 7.22 |
| AN4 | CSF | 0.49 | 0.14 | 0.67 | 1.54 | 1.53 | 1.21 |
| | GM | 65.82 | 895.11 | 0.47 | 13.12 | 12.33 | 10.03 |
| | WM | 37.26 | 1340.49 | 0.72 | 15.84 | 14.96 | 12.96 |
| | Tumor | 151.10 | 829.26 | 0.22 | 12.21 | 11.79 | 7.22 |
| AN5 | CSF | 0.45 | 0.15 | 0.68 | 1.66 | 1.48 | 1.18 |
| | GM | 67.55 | 938.78 | 0.47 | 13.29 | 12.39 | 10.03 |
| | WM | 36.24 | 1355.65 | 0.72 | 15.95 | 15.15 | 12.96 |

| Image No. | Tissue | Feature Values | | | | | |
|-----------|--------|----------------|---------|------|---------|--------|-------|
| | | Mean | Var | Ent | Energy | | |
| | | | | | Hori.z. | Verti. | Diag. |
| | Tumor | 180.57 | 925.29 | 0.17 | 12.48 | 11.41 | 7.51 |
| AN6 | CSF | 0.46 | 0.15 | 0.71 | 1.51 | 1.55 | 1.34 |
| | GM | 66.23 | 899.19 | 0.47 | 13.01 | 12.54 | 9.99 |
| | WM | 36.67 | 1348.12 | 0.73 | 15.69 | 15.26 | 12.91 |
| | Tumor | 151.00 | 906.38 | 0.24 | 11.97 | 12.10 | 8.06 |
| N1 | CSF | 0.53 | 0.14 | 0.67 | 1.52 | 1.5 | 1.19 |
| | GM | 54.40 | 430.72 | 0.4 | 10.79 | 10.48 | 8.18 |
| | WM | 24.21 | 825.47 | 0.74 | 14.34 | 13.84 | 11.84 |
| | Tumor | 41.38 | 4272.17 | 0.67 | 23.31 | 11.75 | 8.11 |
| N2 | CSF | 0.22 | 0.13 | 0.62 | 1.5 | 1.52 | 1.43 |
| | GM | 75.30 | 397.43 | 0.26 | 10.27 | 10.79 | 7.56 |
| | WM | 28.22 | 1077.17 | 0.73 | 15.29 | 15.27 | 12.83 |
| | Tumor | 91.16 | 2965.07 | 0.65 | 18.32 | 21.57 | 18.55 |
| N3 | CSF | 0.28 | 0.14 | 0.73 | 1.53 | 1.52 | 1.37 |
| | GM | 86.64 | 1044.9 | 0.37 | 12.58 | 13.06 | 9.84 |
| | WM | 52.44 | 2138.11 | 0.71 | 17.67 | 18.05 | 14.80 |
| | Tumor | 82.07 | 2187.05 | 0.60 | 16.65 | 16.37 | 13.67 |
| N4 | CSF | 0.53 | 0.12 | 0.62 | 1.37 | 1.43 | 1.17 |
| | GM | 59.09 | 380.3 | 0.36 | 10.42 | 11.21 | 8.00 |
| | WM | 26.17 | 750.23 | 0.73 | 13.57 | 13.93 | 11.57 |
| | Tumor | 71.41 | 3648.76 | 0.73 | 20.56 | 17.98 | 19.37 |

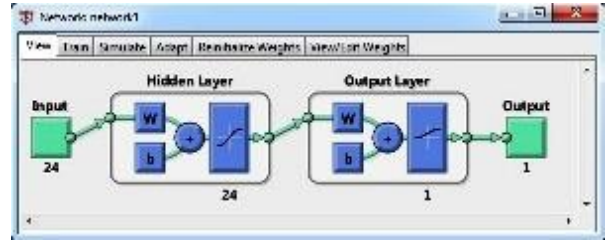


Figure 8 : Structure of MLPNN

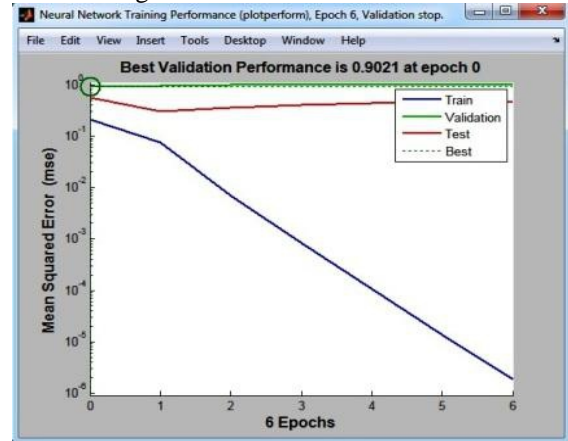


Figure 9: Performance validation of MLPNN

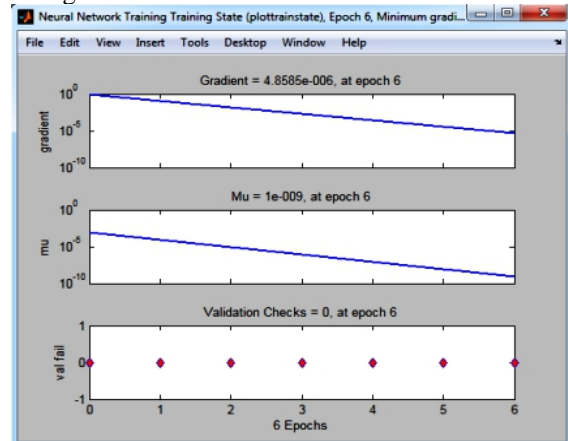


Figure 10: MLPNN training state

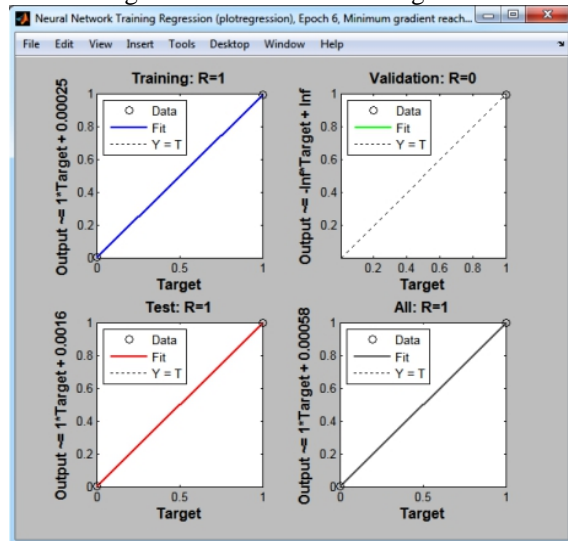


Figure 11: MLPNN training Regression plot

The segmentation result is evaluated with the help of quality rate given as follows,

$$\text{Quality rate, } q_r = \text{area}(A \cap B) / \text{area}(A \cup B) \quad (13)$$

The evaluation of brain tumor detection in different images is carried out using the following metrics,

$$\text{Sensitivity} = TP / (TP + FN) \quad (14)$$

$$\text{Specificity} = TN / (TN + FP) \quad (15)$$

$$\text{Accuracy} = (TN + TP) / (TN + TP + FN + FP) \quad (16)$$

Where, TP stands for True Positive, TN stands for True Negative, FN stands for False Negative and FP stands for False Positive. Table 2 defining the relevant terms of the evaluation metrics like TP, FP, FN, and TN.

TABLE II
Table defining the terms TP, FP, FN, TN

| Experimental Outcome | Condition | | Row Total |
|----------------------|-----------|----------|---------------|
| | Positive | Negative | |
| Positive | TP | FP | TP+FP |
| Negative | FN | TN | FN + TN |
| Column total | TP+FN | FP+TN | N=TP+TN+FP+FN |

With the aid of the input MRI image training and testing dataset, the values of TP, FP, FN, TN, Sensitivity, specificity and accuracy are given in table III & IV. The results show that the accuracy is 83.33%. The evaluation metrics are also compared with the standard methods like KNN and neural network combined with FCM. The evaluation metrics table shows that our proposed method is more accurate than other two methods.

TABLE III
Detection accuracy of the proposed method in training dataset

| Evaluation Metrics | Proposed Method | KNN | FCM + NN |
|--------------------|-----------------|--------|----------|
| True Negative | 43 | 41 | 42 |
| False Positive | 0 | 2 | 2 |
| True Positive | 16 | 15 | 12 |
| False Negative | 1 | 2 | 4 |
| Specificity | 100.00% | 95.35% | 95.45% |
| Sensitivity | 94.12% | 88.24% | 75.00% |
| Accuracy | 98.33% | 93.33% | 90.00% |

TABLE IV
Detection accuracy of the proposed method in testing dataset

| Evaluation Metrics | Proposed Method | KNN | FCM + NN |
|--------------------|-----------------|--------|----------|
| True Negative | 50 | 46 | 46 |
| False Positive | 10 | 13 | 15 |
| True Positive | 25 | 22 | 25 |
| False Negative | 5 | 9 | 4 |
| Specificity | 83.33% | 77.97% | 75.41% |
| Sensitivity | 83.33% | 70.97% | 86.21% |
| Accuracy | 83.33% | 75.56% | 78.89% |

The experimental results for normal and abnormal classification are listed in table III and IV. In the second step, a MLBPNN was used to classify the abnormal image as benign or malignant. The results for benign or

malignant are tabulated in table V.

TABLE V
Tumour Classification

| Type | Benign | Malignant |
|-----------|--------|-----------|
| Benign | 39 | 2 |
| Malignant | 1 | 29 |

VI. CONCLUSION

In this paper, we have presented an effective neural network classifier to identify normal and abnormal (Benign or Malignant) brain images. We have taken 150 images (40 normal, 60 malignant and 50 Benign). The performance of the proposed technique is evaluated by means of the evaluation metrics namely, Sensitivity, Specificity and Accuracy. The comparative analysis is also carried out with KNN and FCM+NN. The obtained result shows that the proposed method produces better results than the other classifiers.

REFERENCES

- [1] Selvaraj.,D., Dhanasekaran,R., “ Novel approach for segmentation of brain magnetic resonance imaging using intensity based thresholding”, 2010 IEEE international conference on communication control and computing technologies, pp 502-507, 7-9 october 2010.
- [2] Selvaraj.,D., Dhanasekaran,R., “ Segmenting internal brain nuclei in MRI brain image using morphological operators”, 2010 International conference on computational intelligence and software engineering, pp 1-4, 10-12 December 2010.
- [3] C. A. Parra, K. Iftexharuddin and R. Kozma, “Automated brain data segmentation and pattern recognition using ANN,” in the Proceedings of the Computational Intelligence, Robotics and Autonomous Systems (CIRAS 03), December, 2003.
- [4] I. Middleton and R. Dampier, “Segmentation of Magnetic Resonance Images using a combination of Neural Networks and Active Contour Models,” in Medical Engineering & Physics, No. 26, pp. 71-86, 2004.
- [5] Zavaljevski, A. Dhawan, A.P. Gaskil, M. Ball, W. and Johnson, J.D., “Multi-level adaptive segmentation of multiparameter MR brain images”, Comput Med Imag Graphics, vol. 24, pp. 87–98, 2000.
- [6] Suckling, J. Sdsson, T. Greenwood, K. and Bullmore, E.T., “A modified fuzzy clustering:

- algorithm for operator independent brain tissue classification of dual echo MR images”, *Magn. Reson. Imag.*, vol. 17, pp. 1065–1076. 1999.
- [7] Alirezaire, J. Jernigan, M.E. and Nahmias, C., “Automatic segmentation of cerebral MR images using artificial neural networks”, *IEEE Trans Nucl Sci*, vol. 45, pp. 2174–2182, 1998.
- [8] Nakazawa, Y. and Saito, T. Region extraction with standard brain atlas for analysis of MRI brain images”, *Proceedings of the IEEE International Conference on Image Process*, vol.1, pp. 387–91, 1994.
- [9] Clark, M.C. Hall, L.C. Goldgof, D.B. Velthuisen, R. Murtagh, F.R. and Silbiger, S., “Automatic tumor segmentation using knowledge-based techniques”, *IEEE Trans. Med. Imag.*, vol. 17, pp. 187–201. 1998.
- [10] Duta, N. and Sonka, M., “Segmentation and interpretation of MR brain images: an improved active shape model”, *IEEE Trans. Med. Imag.*, Vol. 16, pp. 1049–1062, 1998.
- [11] Suri, J., “Two-dimensional fast Magnetic Resonance brain segmentation”, *IEEE Eng Med Biol*, pp. 84–95, 2001.
- [12] Chen, Y. Dougherty, E.R. Totterman, S.M. and Hornak, J.P., “Classification of trabecular structure in magnetic resonance images based on morphological granulometries”, *Magn. Reson. Med*, vol. 29, pp. 358–370, 1993.
- [13] Antalek, B. Hornak, J.P. and Windig, W., “Multivariate image analysis of magnetic resonance images with the direct exponential curve resolution algorithm (DECRA). Part 2. Application to human brain images”, *J. Magn. Reson.*, vol. 132, pp. 307–315. 1998.
- [14] Andersen, A.H. Zhang, Z. Avison, M.J. and Gash, D.M., “Automated segmentation of multispectral brain MR images”, *J. Neurosci Methods*, vol. 122, pp. 13–23. 2002.
- [15] T.K. Moon, “The Expectation Maximization Algorithm”, *IEEE Signal processing magazine*, 1996.
- [16] T. Logeswari and M. Karnan, "An improved implementation of brain tumor detection using segmentation based on soft computing", *Journal of Cancer Research and Experimental Oncology* Vol. 2, No: 1, pp. 006-014, March, 2010.
- [17] A.W. Toga, P. M. Thompson, M. S. Mega, K. L. Narr, R. E. Blanton, “Probabilistic approaches for atlas normal and disease-specific brain variability, *Anatomy and Embryology*”, Vol: 204, No: 4, pp: 267–282, 2001
- [18] “Regionprops Algorithm” from <http://www.mathworks.in/help/toolbox/images/ref/regionprops.html>
- [19] Carlos A. Parra, Khan Iftekharuddin and Robert Kozma, “Automated Brain Data Segmentation and Pattern Recognition Using ANN”, *Computational Intelligence, Robotics and Autonomous Systems (CIRAS 03)*, December 2003
- [20] D. Selvaraj, R. Dhanasekaran, “Segmentation of cerebrospinal fluid and internal brain nuclei in brain magnetic resonance images,” *IRECOS*, Vol.8, issue 5, 2013, pp.1063-1071

